Published in final edited form as:
Science. 2013 September 27; 341(6153): 1517–1521. doi:10.1126/science.1241812.

The Inhibitory Circuit Architecture of the Lateral Hypothalamus Orchestrates Feeding

Joshua H. Jennings[1,2], **Giorgio Rizzi**[1,3], **Alice M. Stamatakis**[1,2], **Randall L. Ung**[1], and **Garret D. Stuber**[1,2,4,5,6,#]

[1]Department of Psychiatry University of North Carolina at Chapel Hill Chapel Hill, NC 27599, U.S.A.

[2]Neurobiology Curriculum University of North Carolina at Chapel Hill Chapel Hill, NC 27599, U.S.A.

[3]University Medical Center Utrecht University of North Carolina at Chapel Hill Chapel Hill, NC 27599, U.S.A.

[4]Bowles Center for Alcohol Studies University of North Carolina at Chapel Hill Chapel Hill, NC 27599, U.S.A.

[5]Neuroscience Center University of North Carolina at Chapel Hill Chapel Hill, NC 27599, U.S.A.

[6]Department of Cell Biology and Physiology University of North Carolina at Chapel Hill Chapel Hill, NC 27599, U.S.A.

Abstract

The growing prevalence of overeating disorders is a key contributor to the worldwide obesity epidemic. Dysfunction of particular neural circuits may trigger deviations from adaptive feeding behaviors. The lateral hypothalamus (LH) is a crucial neural substrate for motivated behavior including feeding, but the precise functional neurocircuitry that controls LH neuronal activity to engage feeding has not been defined. We observed that inhibitory synaptic inputs from the extended amygdala preferentially innervate and suppress the activity of LH glutamatergic neurons to control food intake. These findings help explain how dysregulated activity at a number of unique nodes can result in a cascading failure within a defined brain network to produce maladaptive feeding.

Over half a century ago, experiments in rodents and other species have revealed that gross neuroanatomical manipulations of the LH alter diverse behaviors, including feeding (1–3). While direct anatomical and neuropharmacological manipulations (4, 5) within the LH produce profound alterations in a variety of motivated behaviors, they provide limited mechanistic insight into the discrete circuit connections within the LH that regulate precise behaviors such as feeding. Given the circuit complexity within the LH (6), we aimed to dissect the neurocircuitry between the LH and a principal afferent from the extended amygdala.

[#]To whom correspondence should be addressed. gstuber@med.unc.edu.

The bed nucleus of the stria terminalis (BNST), a neural component of the extended amygdala (7), is a key integrator of diverse motivational states through its interactions with various synaptic targets, including the ventral tegmental area (VTA) (8) and the LH (9). The BNST is comprised primarily of GABAergic cells (10) and consumption of food activates BNST neurons (11). Therefore, we considered the BNST and its inhibitory projections to the LH as an important candidate for regulating feeding. We targeted a Cre-inducible viral construct coding for Channelrhodopsin-2 fused to enhanced yellow fluorescent protein (ChR2-eYFP) into the BNST of *Vgat-ires-Cre* mice and positioned optical fibers above the LH for *in vivo* photostimulation of $Vgat^{BNST\rightarrow LH}$ projection fibers (Fig. 1, A to E and fig. S1). Optogenetic activation of this inhibitory pathway rapidly produced voracious feeding behavior in well-fed mice (Fig. 1, F to I, and fig. S2 and movie S1). We explored the motivational valence of this pathway by testing mice in real-time place preference and self-stimulation assays (Supplementary Methods). $Vgat^{BNST\rightarrow LH}$: :ChR2 mice exhibited a significant place preference for a photostimulation-paired chamber (Fig. 1J and fig. S2) and actively nose poked for photoactivation of the circuit. Food deprivation significantly augmented, while satiety significantly attenuated $Vgat^{BNST\rightarrow LH}$: :ChR2 self-stimulation (Fig. 1K and fig. S2). The evoked feeding response was specific to the $Vgat^{BNST\rightarrow LH}$ pathway. Photoactivation of $Vgat^{BNST\rightarrow VTA}$ projections did not elicit feeding behavior (figs. S3 and S4).

Because high-caloric diets can facilitate overeating (12), we determined whether consumption induced by $Vgat^{BNST\rightarrow LH}$ circuit activation was directed towards palatable energy-dense foods (Supplementary Methods). Well-fed $Vgat^{BNST\rightarrow LH}$: :ChR2 mice showed a strong preference for high-fat food during photostimulation exposure (table S1 and movie S1), suggesting that activation of the $Vgat^{BNST\rightarrow LH}$ circuit is sufficient for eliciting feeding that is preferential for calorie-dense substances even when energy requirements are satisfied.

To examine whether endogenous activity of the $Vgat^{BNST\rightarrow LH}$ pathway is important for feeding, we transduced BNST-GABAergic neurons (Fig. 2A) and their axons that innervate the LH (Fig. 2B and fig. S5) with the inhibitory opsin, archaerhodopsin (eArch3.0-eYFP) (13, 14). Suppression of presynaptic BNST-GABAergic signaling via eArch3.0 activation resulted in enhanced LH-postsynaptic neuronal activity during anesthetized extracellular recordings (Fig. 2, C to E). Despite the influence of hunger, photoinhibition of the $Vgat^{BNST\rightarrow LH}$ circuit reduced feeding in food-deprived mice (Fig. 2, F to J, and fig. S6). Furthermore, photoinhibition of $Vgat^{BNST\rightarrow LH}$ projections led to a significant avoidance of a photoinhibition-paired chamber (Fig. 2K and fig. S6).

The hypothalamus contains numerous genetically distinct neuronal populations (15–21). We thus characterized the molecular phenotype of the postsynaptic LH neuronal targets that receive functional $Vgat^{BNST\rightarrow LH}$ innervation. We paired photostimulation of $Vgat^{BNST\rightarrow LH}$ inputs with whole-cell recordings in conjunction with multiplexed gene expression profiling of individual LH neurons in brain slices (Fig. 3A, Supplementary Methods). We focused on a set of genes known to be heterogeneously expressed in the LH and whose products have been implicated in feeding (22). BNST-GABAergic inputs formed strong functional connections with postsynaptic LH neurons that expressed significantly higher levels of

Vglut2. In contrast, weakly innervated LH neurons displayed significantly lower levels of *Vglut2* and higher levels of *Vgat* expression (Fig. 3, B and C, and fig. S7, and table S2).

We confirmed these findings by utilizing modified rabies virus tracing techniques to identify the monosynaptic inputs to glutamatergic and GABAergic neurons in the LH (Fig. 3D). In *Vglut2-ires-Cre* and *Vgat-ires-Cre* mice, we targeted Cre-inducible TVA (AAV5-FLEX-TVA-mCherry) and RG (AAV8-FLEX-RG) proteins that allow for rabies virus infection and subsequent transsynaptic viral propagation, respectively (23, 24), to LH-glutamatergic or -GABAergic neurons. Two weeks after AAV transduction, the modified rabies virus, SADΔG-GFP(EnvA), was injected into the LH, and BNST-containing slices were obtained 7 days later for confocal imaging. *Vglut2*^{LH}: :Rabies tracing revealed dense populations of transsynaptically labeled BNST neurons (Fig. 3, E and F), while *Vgat*^{LH}: :Rabies tracing resulted in minimal BNST labeling (Fig. 3, G to I, and fig. S8).

Because BNST-GABAergic projection neurons promote feeding and selectively target LH glutamatergic neurons, we considered *Vglut2*^{LH} neurons as a critical downstream circuit node for regulating food intake. Photoactivation of *Vglut2*^{LH} neurons (Fig. 4A and fig. S9) suppressed feeding in food-deprived mice (Fig. 4, B to F, and fig. S10), while photoinhibition of *Vglut2*^{LH} neurons induced feeding in well-fed mice (figs. S11 to S13). Photostimulation of *Vglut2*^{LH} neurons produced aversion (Fig. 4G and fig. S10) and *Vglut2*^{LH} inhibition produced a preference for palatable foods (table S1).

Until now, the precise neurocircuit elements responsible for the feeding and reinforcement phenomena observed five decades ago by electrical stimulation of the LH (1, 2, 25) have remained a mystery. Inhibitory inputs from the BNST specifically innervate and suppress LH glutamatergic neurons to promote feeding. Further unraveling of the specific patterns of gene expression and projection targets of LH glutamatergic neurons could identify novel points for therapeutic intervention within these circuits for the treatment of eating disorders and obesity.

Supplementary Material

Refer to Web version on PubMed Central for supplementary material.

Acknowledgments

We thank the Stuber lab and Dr. Cynthia Bulik for discussion. We thank Drs. Karl Deisseroth and Ed Boyden for viral constructs and the UNC vector core for viral packaging, Drs. Bradford Lowell and Linh Vong for mice, and the UNC Neuroscience Center Microscopy Core (P30 NS045892). This study was supported by The Klarman Family Foundation, The Brain and Behavior Research Foundation, The Foundation of Hope, and the National Institute on Drug Abuse (DA032750) (G.D.S.). A.M.S. was supported by (NS007431 and DA034472).

References and Notes

1. Hoebel BG, Teitelbaum P. Hypothalamic Control of Feeding and Self-Stimulation. Science. 1962; 135:375–377. [PubMed: 13907995]
2. Delgado JR, Anand BK. Increase of food intake induced by electrical stimulation of the lateral hypothalamus. Am. J. Physiol. 1953; 172:162–168. [PubMed: 13030733]

3. Wise RA. Hypothalamic motivational systems: fixed or plastic neural circuits? Science. 1968; 162:377–379. [PubMed: 5677536]
4. Stanley BG, Ha LH, Spears LC, Dee MG 2nd. Lateral hypothalamic injections of glutamate, kainic acid, D,L-alpha-amino-3-hydroxy-5-methyl isoxazole propionic acid or N-methyl-D-aspartic acid rapidly elicit intense transient eating in rats. Brain Res. 1993; 613:88–95. [PubMed: 7688643]
5. Turenius CI, et al. GABA(A) receptors in the lateral hypothalamus as mediators of satiety and body weight regulation. Brain Res. 2009; 1262:16–24. [PubMed: 19401161]
6. Hahn JD, Swanson LW. Connections of the lateral hypothalamic area juxtadorsomedial region in the male rat. J. Comp. Neurol. 2012; 520:1831–1890. [PubMed: 22488503]
7. de Olmos JS, Heimer L. The concepts of the ventral striatopallidal system and extended amygdala. Ann. N. Y. Acad. Sci. 1999; 877:1–32. [PubMed: 10415640]
8. Jennings JH, et al. Distinct extended amygdala circuits for divergent motivational states. Nature. 2013; 496:224–228. [PubMed: 23515155]
9. Kim S-Y, et al. Diverging neural pathways assemble a behavioural state from separable features in anxiety. Nature. 2013; 496:219–223. [PubMed: 23515158]
10. Kudo T, et al. Three types of neurochemical projection from the bed nucleus of the stria terminalis to the ventral tegmental area in adult mice. J. Neurosci. Off. J. Soc. Neurosci. 2012; 32:18035–18046.
11. Ángeles-Castellanos M, Mendoza J, Escobar C. Restricted feeding schedules phase shift daily rhythms of c-Fos and protein Per1 immunoreactivity in corticolimbic regions in rats. Neuroscience. 2007; 144:344–355. [PubMed: 17045749]
12. Johnson PM, Kenny PJ. Dopamine D2 receptors in addiction-like reward dysfunction and compulsive eating in obese rats. Nat. Neurosci. 2010; 13:635–641. [PubMed: 20348917]
13. Chow BY, et al. High-performance genetically targetable optical neural silencing by light-driven proton pumps. Nature. 2010; 463:98–102. [PubMed: 20054397]
14. Mattis J, et al. Principles for applying optogenetic tools derived from direct comparative analysis of microbial opsins. Nat. Methods. 2012; 9:159–172. [PubMed: 22179551]
15. Karnani MM, Szabó G, Erdélyi F, Burdakov D. Lateral hypothalamic GAD65 neurons are spontaneously firing and distinct from orexin- and melanin-concentrating hormone neurons. J. Physiol. 2013; 591:933–953. [PubMed: 23184514]
16. Knight ZA, et al. Molecular Profiling of Activated Neurons by Phosphorylated Ribosome Capture. Cell. 2012; 151:1126–1137. [PubMed: 23178128]
17. Leinninger GM, et al. Leptin action via neurotensin neurons controls orexin, the mesolimbic dopamine system and energy balance. Cell Metab. 2011; 14:313–323. [PubMed: 21907138]
18. Sakurai T, et al. Orexins and orexin receptors: a family of hypothalamic neuropeptides and G protein-coupled receptors that regulate feeding behavior. Cell. 1998; 92:573–585. [PubMed: 9491897]
19. Sharf R, et al. Orexin signaling via the orexin 1 receptor mediates operant responding for food reinforcement. Biol. Psychiatry. 2010; 67:753–760. [PubMed: 20189166]
20. Swanson LW, Sanchez-Watts G, Watts AG. Comparison of melanin-concentrating hormone and hypocretin/orexin mRNA expression patterns in a new parceling scheme of the lateral hypothalamic zone. Neurosci. Lett. 2005; 387:80–84. [PubMed: 16084021]
21. Atasoy D, Betley JN, Su HH, Sternson SM. Deconstruction of a neural circuit for hunger. Nature. 2012; 488:172–177. [PubMed: 22801496]
22. Berthoud H-R, Münzberg H. The lateral hypothalamus as integrator of metabolic and environmental needs: from electrical self-stimulation to optogenetics. Physiol. Behav. 2011; 104:29–39. [PubMed: 21549732]
23. Watabe-Uchida M, Zhu L, Ogawa SK, Vamanrao A, Uchida N. Whole-brain mapping of direct inputs to midbrain dopamine neurons. Neuron. 2012; 74:858–873. [PubMed: 22681690]
24. Wickersham IR, Finke S, Conzelmann K-K, Callaway EM. Retrograde neuronal tracing with a deletion-mutant rabies virus. Nat. Methods. 2007; 4:47–49. [PubMed: 17179932]
25. Olds J, Milner P. Positive reinforcement produced by electrical stimulation of septal area and other regions of rat brain. J. Comp. Physiol. Psychol. 1954; 47:419–427. [PubMed: 13233369]

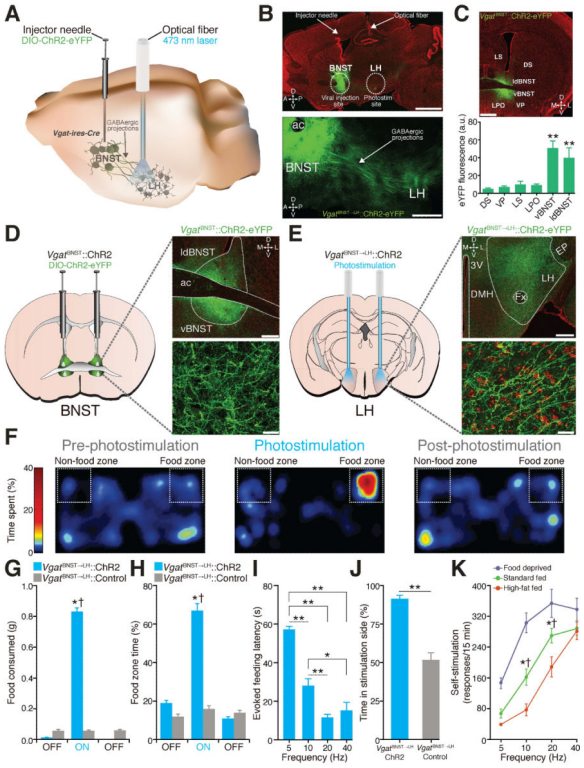

Fig. 1. *Vgat*$^{\mathbf{BNST\rightarrow LH}}$ circuit activation induces feeding in well-fed mice

(**A**) *Vgat*$^{\mathrm{BNST\rightarrow LH}}$ circuit targeting. (**B**) 10x (top) and 20x (bottom) images of the *Vgat*$^{\mathrm{BNST\rightarrow LH}}$::ChR2-eYFP circuit (scale bars = 1 mm (top), 500 μm (bottom)). (**C**) Localized ChR2-eYFP expression in the BNST (top) and quantified eYFP fluorescence intensity (bottom) is significantly greater in the BNST compared to surrounding regions ($F_{5,29}$ = 11.22, P < 0.001, n = 5 sections from n = 5 mice; ac, anterior commissure; ldBNST, lateral-dorsal BNST; vBNST, ventral BNST; LS, lateral septum; LPO, lateral preoptic area; VP, ventral pallidum; DS, dorsal striatum; scale bar = 200 μm). (**D** and **E**) ChR2-eYFP expression in the BNST (D) and axonal projections in the LH (E) in *Vgat-ires-Cre* mice (LH, lateral hypothalamus; Fx, fornix; EP, entopeduncular nucleus; DMH, dorsomedial hypothalamus; 3V, third ventricle; D, dorsal; V, ventral; L, lateral; M, medial; green = ChR2-eYFP; red = Nissl stain; scale bars = 200 μm (top), 20 μm (bottom)). (**F**) Spatial location heat maps in 20 min epochs before, during, and after 20-Hz photostimulation-induced feeding. (**G** and **H**) Photostimulation of *Vgat*$^{\mathrm{BNST\rightarrow LH}}$ projections significantly increased grain-based (standard) food intake ($F_{2,24}$ = 201.6, P < 0.001) (G) and food zone time ($F_{2,24}$ = 18.61, P < 0.001, n = 5 mice per group) (H). (**I**) Higher photostimulation frequencies significantly decreased evoked feeding latencies ($F_{3,56}$ = 48.89, P < 0.001, n = 9 mice). (**J**) *Vgat*$^{\mathrm{BNST\rightarrow LH}}$::ChR2 mice spent significantly more time in the photostimulation-paired side compared to controls (P < 0.001, n = 5 mice per group). (**K**) Food-deprived *Vgat*$^{\mathrm{BNST\rightarrow LH}}$::ChR2 mice nose poked significantly more for 10- and 20-Hz photostimulation when compared to 2 days of standard fed *ad libitum* and to 2 days of standard fed *ad libitum* supplemented with 2 hr of high-fat food exposure before the self-stimulation session (F2,204 = 40.87, P < 0.001, n = 9 mice). All values for all figures

represent mean ± s.e.m. * $P < 0.05$, ** $P < 0.001$ (Student's t-test or ANOVA followed by Bonferroni post-hoc comparisons, where applicable). Dagger symbol denotes significance compared to all manipulations.

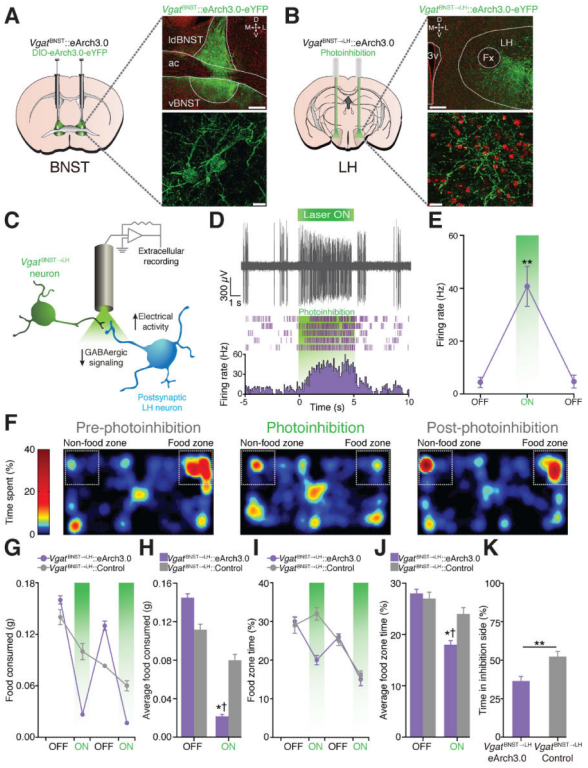

Fig. 2. *Vgat*$^{\mathbf{BNST\rightarrow LH}}$ circuit inhibition diminishes feeding in food-deprived mice and is aversive

(**A** and **B**) eArch3.0-eYFP expression in the BNST (A) and axonal projections in the LH (B) in *Vgat-ires-Cre* mice (scale bars = 200 μm (top), 20 μm (bottom)). (**C**) Schematic for anesthetized *in vivo* extracellular recordings in the LH. (**D**) Example trace from a single LH unit (top) and its representative peri-event histogram and raster (bottom). (**E**) The average firing rate of light-responsive LH units significantly increased during the 5-s photoinhibition trials ($F_{2,12}$ = 19.52, P < 0.001, n = 5 units from n = 3 mice). (**F**) Spatial location heat maps in 10 min epochs before, during, and after photoinhibition. (**G** and **H**) Photoinhibition of *Vgat*$^{\mathrm{BNST\rightarrow LH}}$ projections significantly decreased standard food intake ($F_{1,44}$ = 16.30, P < 0.001) and time spent in the food zone (**I** and **J**) ($F_{1,44}$ = 2.43, P = 0.028, n = 6 mice per group). (**K**) *Vgat*$^{\mathrm{BNST\rightarrow LH}}$::eArch3.0 mice spent significantly less time in the photoinhibition-paired side when compared to controls (P = 0.004, n = 6 mice per group).

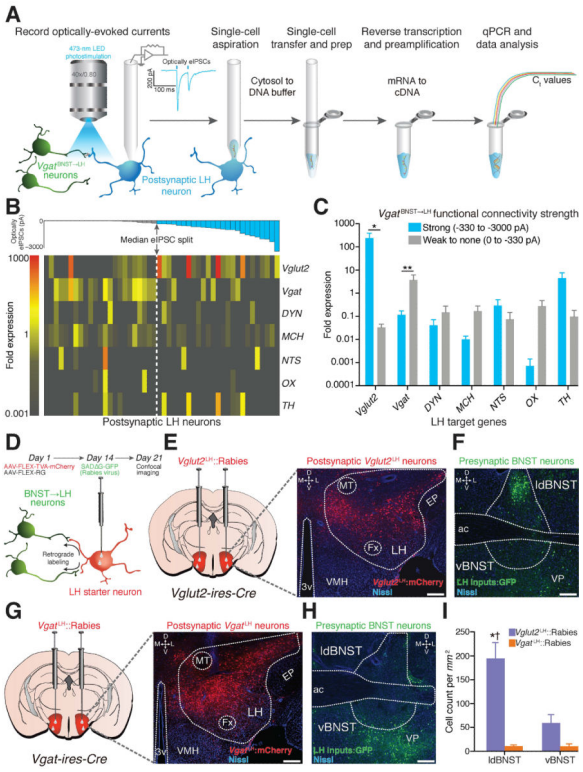

Fig. 3. *Vgat*$^{\mathbf{BNST\rightarrow LH}}$ projections preferentially target LH glutamatergic neurons

(**A**) Schematic for ChR2-assisted circuit mapping with single-cell gene expression profiling. (**B**) Color-coded fold expression of all target genes from all recorded LH neurons (*Vglut2*, vesicular glutamate transporter-2; *Vgat*, vesicular GABA transporter; *DYN*, dynorphin; *MCH*, melanin-concentrating hormone; *NTS*, neurotensin; *OX*, orexin/hypocretin; *TH*, tyrosine hydroxylase). The average fold expression for *Vglut2* was significantly higher in postsynaptic LH neurons that display large optically-evoked inhibitory postsynaptic current amplitudes (strongly innervated) compared to weakly innervated LH neurons ($U = 169.0$, $P = 0.016$, $n = 6$ mice, $n = 48$ cells). (**D**) Schematic for modified rabies virus tracing. (**E** and **F**) Images from a *Vglut2-ires-cre* mouse showing FLEX-TVA-mCherry expression in LH glutamatergic neurons (E) and appreciable SADΔG-GFP labeling of BNST neurons (F). (**G** and **H**) FLEX-TVA-mCherry expression in LH GABAergic neurons (G) and minimal SADΔG-GFP labeling of BNST neurons (H) (green = SADΔG-GFP; red = FLEX-TVA-mCherry; blue = Nissl stain; scale bars = 200 μm). (**I**) Significantly more BNST neurons innervate LH glutamatergic neurons compared to LH GABAergic neurons ($F_{1,20} = 38.50$, $P < 0.001$, $n = 3$ mice per group).

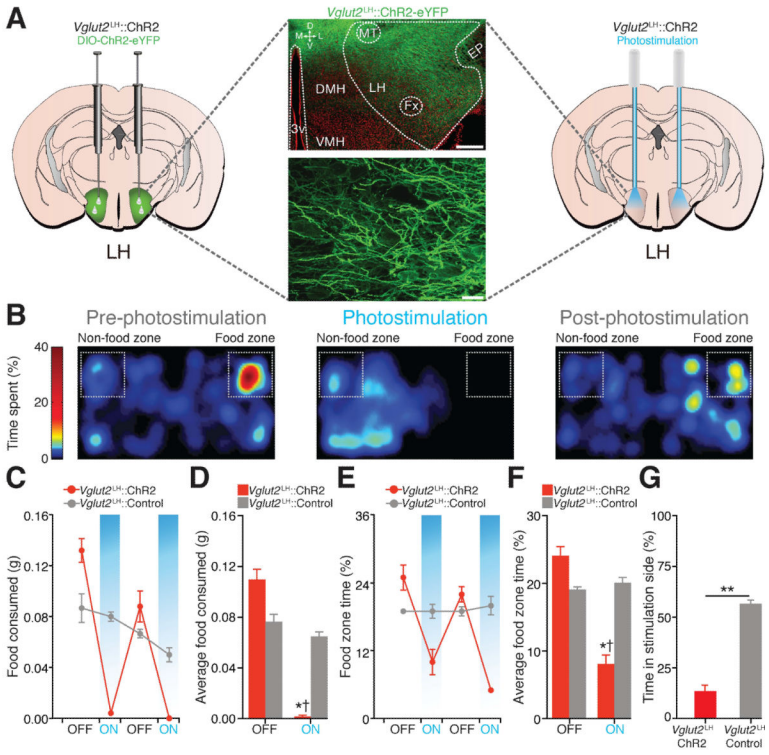

Fig. 4. Photoactivation of *Vglut2*^{LH} neurons suppresses feeding in food-deprived mice and is aversive

(**A**) ChR2-eYFP expression in the LH of a *Vglut2-ires-Cre* mouse (scale bars = 200 μm (top), 20 μm (bottom)). (**B**) Spatial location heat maps in 10 min epochs before, during, and after 5-Hz photostimulation. (**C** and **D**) Photostimulation of *Vglut2*^{LH} neurons significantly decreased food intake ($F_{1,36}$ = 13.31, $P < 0.001$) and food zone time (**E** and **F**) ($F_{1,36}$ = 13.12, $P < 0.001$, n = 5 mice per group). (**G**) *Vglut2*^{LH}::ChR2 mice spent significantly less time in the photostimulation-paired side when compared to controls ($P < 0.001$, n = 5 mice per group).